Available online at www.sciencedirect.com
ScienceDirect
Trans. Nonferrous Met. Soc. China 25(2015) 4018−4027
Transactions of Nonferrous Metals Society of China
www.tnmsc.cn

In vitro biodegradability and biocompatibility of porous Mg−Zn scaffolds coated with nano hydroxyapatite via pulse electrodeposition

Z. S. SEYEDRAOUFI, Sh. MIRDAMADI

School of Metallurgy and Materials Engineering, Iran University of Science and Technology, Tehran 16846-13114, Iran

Received 26 January 2015; accepted 17 June 2015

Abstract: The biodegradability and biocompatibility of porous Mg−2Zn (mass fraction, %) scaffolds coated with nano hydroxyapatite (HAP) were investigated. The nano HAP coating on Mg−2Zn scaffolds was prepared by the pulse electrodeposition method. The as-deposited scaffolds were then post-treated with alkaline solution to improve the biodegradation behavior and biocompatibility for implant applications. The microstructure and composition of scaffold and nano HAP coating, as well as their degradation and cytotoxicity behavior in simulated body fluid (SBF) were investigated. The post-treated coating is composed of needle-like HAP with the diameter less than 100 nm developed almost perpendicularly to the substrate, which exhibits a similar composition to natural bone. It is found that the products of immersion in SBF are identified to be HAP, $(Ca,Mg)_3(PO_4)_2$ and $Mg(OH)_2$. The bioactivity, biocompatibility and cell viabilities for the as-coated and post-treated scaffold extracts are higher than those for the uncoated scaffold. MG63 cells are found to adhere and proliferate on the surface of the as-coated and post-treated scaffolds, making it a promising choice for medical application. The results show that the pulse electrodeposition of nano HAP coating and alkaline treatment is a useful approach to improve the biodegradability and bioactivity of porous Mg−Zn scaffolds.
Key words: porous Mg−Zn scaffold; hydroxyapatite coating; pulse electrodeposition; biodegradability; biocompatibility

1 Introduction

Tissue engineering seeks to improve the regeneration ability of host tissue through a designed scaffold that is populated with cells and signaling molecules [1]. Bone tissue engineering has the potential to become a real alternative to autologous bone grafts. In order to be compatible with the complex biological system of the human body, the requirements of ideal scaffolds for bone tissue engineering are summarized as follows.

First, scaffolds must be biocompatible and should degrade into nontoxic components. In addition, scaffolds must possess enough mechanical properties matching those of the host bone and not collapse during the period of handling and normal activities of the patient. A further requirement for scaffolds is a controllable interconnected high porosity for cell seeding and ingrowth as well as a pore size within a range of 300−400 μm. Other desirable features of scaffolds are excellent osteoconductivity and good biodegradability. Today, materials used as bone tissue engineering scaffolds are mainly bioactive ceramics, natural or synthetic polymers, and composites of polymers and ceramics. Although some encouraging results have been reported, these materials suffer from limitations on the application. For example, the polymers possess very low modulus and strength while the ceramics are very stiff and brittle, thus, they are unsuitable as load-bearing bone substitutes [1−13]. Therefore, it is crucial to develop new scaffolds with better mechanical properties.

It is well known that metals possess the mechanical properties suitable for load-bearing applications. Among them, Mg and its alloys can offer many advantages as a promising biomaterial, e.g., relatively low elastic modulus and proper strength, the density close to that of human bone, excellent biocompatibility, biodegradability and bioresorbability. TAN et al [1] performed outstanding works on open porous Mg scaffolds in vivo. The results showed that Mg scaffolds are very promising candidates for the development of novel implants in musculoskeletal surgery.

Implants made from Mg and Mg alloys degrade more rapidly in physiological environments than in the normal healing process. Mg is extremely susceptible to

Corresponding author: Z. S. SEYEDRAOUFI; Tel: +98-21-77459151; Fax: +98-21-77240480; E-mail: zahraseyedraoufi@iust.ac.ir
DOI: 10.1016/S1003-6326(15)64051-1

degradation because of its high reactivity. The degradation protection provided by the surface oxide layer is limited by its porosity and brittleness, especially in an aqueous environment with chloride ions. Zn element is involved in the synthesis and activities of many enzymes in the body. Insufficient Zn intake reduces DNA duplication and protein synthesis. More importantly, Zn improves the mechanical properties and corrosion resistance of Mg scaffold. A small quantity of Zn in the Mg alloy not only results in alloy strengthening, but also rises the electrical potential of Mg and improves its corrosion resistance [14−18].

Surface treatment is often necessary to control Mg degradation in a rate that matches the tissue growth, in addition to designing Mg alloy composition and processing [14]. Hydroxyapatite (HAP) coatings on the surface of Mg and Mg alloys can also slow down the degradation rate. HAP is the dominant mineral in bone tissue and has good biocompatibility and biological activity [19], and is one of the most frequently used biomaterials for bone repair. HAP cannot support high loads due to its inherent brittleness and low fracture toughness, but can serve as coating material for other load bearing biomaterials. HAP is a promising coating material for orthopedic and craniofacial applications because of its osteogenic properties [14].

Nano HAP coating has structure that is more matched to the bone structure in which the implants should function and have lower sintering temperature [20]. Many methods have already been developed to prepare HAP coatings on metallic substrates, such as sol−gel process, electrophoretic deposition, sputtering process and biomimetic methods. However, these cannot be used to deposit HAP coating on Mg alloy because of its low melting point and poor heat resistance [13,21]. Electrochemical deposition has unique advantages due to its capability of forming a uniform coating on a porous substrate or one with a complex shape, its controllability with regard to the thickness and chemical composition of the coating and its low deposition temperature [13,20,21]. In addition, the morphology of coating can be controlled easily by varying the electrochemical potential and electrolyte concentration [20,22]. It is thus recognized as one of the most promising techniques to produce degradable Mg alloy. Nevertheless, in a traditional cathodic electrodeposition process, when a static potential is applied, loose, porous and low adhesive coatings can be easily developed. In order to solve this problem, it was suggested that pulsed power can be used for deposition of an adherent coating [21,23].

WEN et al [3], ZHUANG et al [2] and SEYEDRAOUFI and MIRDAMADI [24] produced porous Mg and Mg–Zn scaffolds and investigated the mechanical properties of the samples. Compared with the porous bioactive ceramic and polymeric scaffold, the porous Mg and Mg−Zn specimens have proper mechanical properties which are closer to those of natural bone. Furthermore, the porous Mg specimens have changeable in vitro degradable rates, which are enhanced by increasing the porosity [2]. Therefore, it is suggested that the corrosion resistance of Mg scaffolds is improved. Until now, there has not study on in vitro biodegradability and biocompatibility of the porous Mg−Zn scaffolds coated with nano HAP via pulse electrodeposition process. Because the anti-corrosion property of Mg−Zn alloy can be effectively improved by Zn element when the content is less than 3% [17], Mg−2Zn (mass fraction, %) scaffolds are considered as substrate. In the present work, porous Mg−2Zn (mass fraction, %) specimens were fabricated using a powder metallurgy process. Nano HA coating was directly deposited on the porous Mg−2Zn scaffold using the pulse electrodeposition method. The microstructural and compositional changes of HAP coating, as well as the biodegradability and biocompatibility behavior of as-synthesized, as-deposited and post-treated porous Mg−2Zn scaffolds in simulated body fluid (SBF) were investigated.

2 Experimental

2.1 Synthesis of scaffold

Pure Mg (purity ≥99%, particle size ≤100 μm) and pure Zn (purity ≥99.8%, particle size ≤45 μm) powders purchased from Merck were utilized as the starting materials. Carbamide ($CO(NH_2)_2$) particles purchased from Merck were employed as the space-holder agent. The particle size of the spacer agent material was in the range of 200−400 μm with a purity of 99.9%. After mixing the starting materials with the space-holder particles, porous Mg−2Zn specimens were prepared through a powder metallurgy process. The mixtures of Mg and Zn powder were prepared based on the Zn content of 2%, while the carbamide particles were thoroughly added to the above specimens with volume fraction of 15%.

The mixed powder was uniaxially pressed at a pressure of 200 MPa into green compacts with dimensions of 10 mm in diameter and 10 mm in length. The green compacts were subsequently heat treated to burn out the spacer particles and to sinter the porous Mg–Zn specimens separately in a tube furnace under an argon atmosphere. The heat treatment process consisted of two steps: firstly heating up to 250 °C at a rate of 3.75 °C/min and staying for 4 h to burn out the spacer

particles, and then heating up to 550 °C at a rate of 8 °C/min and staying for 2 h to sinter the porous scaffolds. After the sintering stage, the specimens were furnace cooled down to room temperature.

2.2 Coating process

The synthesized Mg−2Zn scaffold was considered the substrate material. During the electrodeposition, the Mg−2Zn alloy sample was used as the working electrode and a cylindrical graphite served as the counter electrode. Before deposition, in order to obtain a clean and fresh working surface, the samples were, sequentially, polished with silicon carbide papers of 400−1000 grits, cleaned ultrasonically in acetone, activated with 10% HNO_3 solution for 10 s, and dried using a drying apparatus. The electrolyte used for deposition of calcium phosphate was prepared by mixing a solution of 0.042 mol/L $Ca(NO_3)_2$, 0.025 mol/L $NH_4H_2PO_4$ and 0.1 mol/L $NaNO_3$. The pH value of the electrolyte was adjusted to 5.0 by dilute HNO_3 and $(CH_2OH)_3CNH_2$ solutions. These reagents were all analytic grade. The deposition was performed with fixed frequency (100 Hz) by pulse peak current density of 40 mA/cm^2 and positive pulse duty cycles of 0.1 at 85 °C for 1 h. When the specimens were coated with calcium phosphate, they were removed from the electrolytic solution, rinsed in distilled water and dried for about 4 h in air. Then, the as-deposited samples under optimum conditions of coating were immersed in 0.25 mol/L NaOH solution at 80 °C for 4 h, rinsed in distilled water and dried at 80 °C for 4 h.

2.3 Characterization

The chemical composition of the scaffold and coatings was detected by X-ray diffraction (XRD) (Philips 1800PW) with Cu K_α radiation. The surface morphology and element composition of scaffold and coatings were identified by scanning electron microscopy (SEM) (Tscan−Vega) equipped with energy dispersion spectroscopy (EDS). The mechanical properties of the porous Mg−2Zn specimens were measured using compression testing of samples with dimensions of d10 mm × 15 mm. The tests were performed with a SANTAM (STM-20, Iran) testing machine at room temperature and a rate of 0.3 mm/s. Each result was taken as the mean value of testing on five samples.

2.4 Immersion testing

The immersion testing was carried out in the SBF solution [25]. The pH value of SBF was adjusted to 7.4 with HCl and $(HOCH_2)_3CNH_2$ solutions, and the temperature was kept at 37 °C using water bath. After different immersion periods, the specimens were removed from SBF, rinsed gently with distilled water and dried at 60 °C by drying apparatus. The composition change of the scaffolds after immersion tests was characterized by XRD. An average of three measurements was used for evaluating the pH value of solutions and the specific mass variations.

2.5 Indirect cytotoxicity measurement

Human osteosarcoma cells (MG63) were used in the vitro cell culture experiment. They were cultured in Dulbecco's modified Eagle's medium (DMEM), 10% fetal bovine serum (FBS), 100 U/mL penicillin and 100 μg/mL streptomycin at 37 °C in a humidified atmosphere of 5% CO_2. The extraction media were prepared using DMEM serum free medium with the surface area/extraction medium ratio of 1 cm^2/mL in a humidified atmosphere with 5% CO_2 at 37 °C for 72 h. The supernatant fluid was withdrawn and centrifuged to prepare the extraction medium, then refrigerated at 4 °C before the cytotoxicity test. The control groups involved the use of DMEM medium as the negative control and 10% dimethyl sulfoxide (DMSO) DMEM medium as the positive control. The cells were incubated in 96-well cell culture plates at 50 cells/μL medium in each well and incubated for 24 h to allow attachment. The medium was then replaced with 100 μL extraction medium. After incubating the cells in a humidified atmosphere with 5% CO_2 at 37 °C for 5 and 10 d, respectively, the 96-well cell culture plates were observed under an optical microscope. After that, 10 μL 3-[4,5-dimethylthiazol-2-yl]-2,5-diphenyltetrazolium bromide (MTT) was added to each well. The samples were incubated with MTT at 37 °C for 4 h, and then 100 μL formazansolubilization solution (10%SDS in 0.01 mol/L HCl) was added in each well overnight in the incubator in a humidified atmosphere. The spectrophotometrical absorbance of the samples was measured by microplate reader (Bio-RAD680) at 570 nm with a reference wavelength of 630 nm.

2.6 Direct cell adhesion experiment

200 μL cell suspension was seeded onto the as-synthesized, as-deposited and post-treated porous Mg−2Zn scaffolds as well as the control sample at a cell density of 5×10^4 cell/mL. After 8 h culture in a humidified atmosphere with 5% CO_2 at 37 °C in 96-well plates, the parallel samples were fixed in 2.5% glutaraldehyde solution for 2 h at room temperature and rinsed 3 times with phosphate buffer solution (PBS, pH= 7.4), followed by dehydration in a gradient ethanol/ distilled water mixture (50%, 60%, 70%, 80%, 90%, 100%) for 10 min each and dried in hexamethyldisilazane (HMDS) solution. The surface of cell adhered experimental samples was observed by SEM.

3 Results and discussion

3.1 Microstructure and composition of scaffold

Figure 1 shows the optical micrograph of porous Mg−2Zn scaffold sintered at 550 °C. It is clear that the pore sizes are 200−400 μm. The black phases correspond to the porosity, while the white phases belong to the Mg matrix. According to Ref. [2], the porosity volume fraction of the scaffold is about 20%. The visual characterisation of the pores revealed that two types of pores, open interconnected macropores and small isolated micropores, are distinguishable within the microstructure of the porous scaffold. Some of the micropores form as a result of volume shrinkage of the Mg and Zn powders during the sintering process.

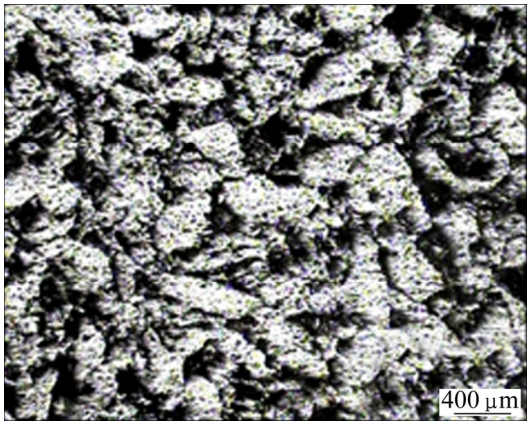

Fig. 1 Optical micrograph of Mg−2Zn scaffold

The XRD pattern of scaffold sintered at 550 °C is shown in Fig. 2. As observed in the pattern, Mg peaks are detected in the sample, and MgO is detected as the minor phase. In fact, the presence of magnesium oxide peaks indicates that MgO most likely forms during the preparation and/or sintering process. However, MgO is a non-toxic oxide biologically [26]. However, the XRD result cannot reveal the presence of any other possible phases. The EDS elemental mappings of the Mg−2Zn scaffold sintered at 550 °C are shown in Fig. 3 and it can be inferred that Zn is uniformly distributed in the Mg matrix.

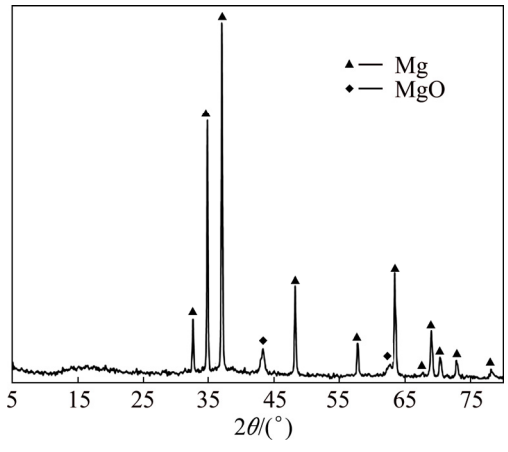

Fig. 2 XRD pattern of Mg−2Zn scaffold

The compressive strength and elastic modulus of the porous Mg−2Zn scaffold are 58 and 6000 MPa, respectively. However, compared with the porous bioactive ceramic and polymeric scaffolds, the porous Mg−Zn specimens have more appropriate mechanical properties that are closer to those of natural bone. Therefore, the porous Mg–Zn metals have the potential to serve as the degradable implants for the bone substitute applications.

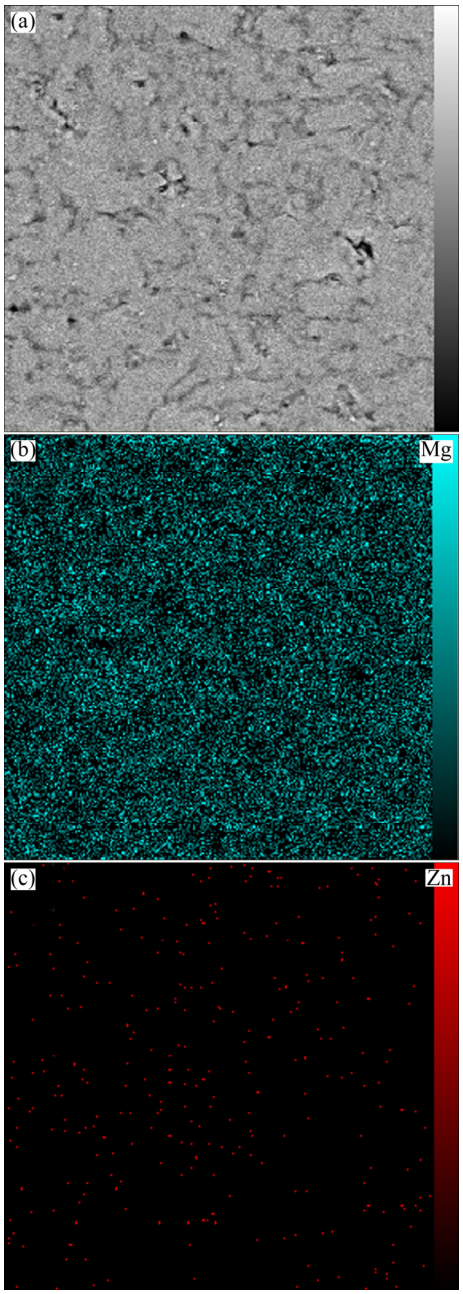

Fig. 3 SEM image (a) and elemental mapping images (b,c) of Mg−2Zn scaffold

3.2 Microstructure and composition of coating

The XRD patterns of the as-deposited and the post-treated coatings (Fig. 4) indicate that during the electrodeposition process, a mixture of $Ca_{10}(PO_4)_6(OH)_2$ (HAP) and $CaHPO_4.2H_2O$ (DCPD) forms in the as-deposited coating. In the electrodeposition process, with applying a high cathode current, the cathodic polarization of the Mg alloy leads to an increase of pH value at the interface between the alloy and the electrolyte due to the formation of OH^- ions. Not only does this sudden increase of pH value trigger crystal nucleation of the desired Ca−P phase directly on the substrate surface but also initiate the Ca−P crystal growth. HAP is the most stable calcium phosphate ceramic under local strong basic conditions. The electrodeposition reactions on the surface of substrate are suggested as follows:

$$2H_2PO_4^-+2e\longrightarrow 2HPO_4^{2-}+H_2\uparrow \quad (1)$$

$$2HPO_4^{2-}+2e\longrightarrow 2PO_4^{3-}+H_2\uparrow \quad (2)$$

$$10Ca^{2+}+6PO_4^{3-}+2OH^-\longrightarrow Ca_{10}(PO_4)_6(OH)_2 \quad (3)$$

$$Ca^{2+}+HPO_4^{2-}+2H_2O\longrightarrow CaHPO_4\cdot 2H_2O \quad (4)$$

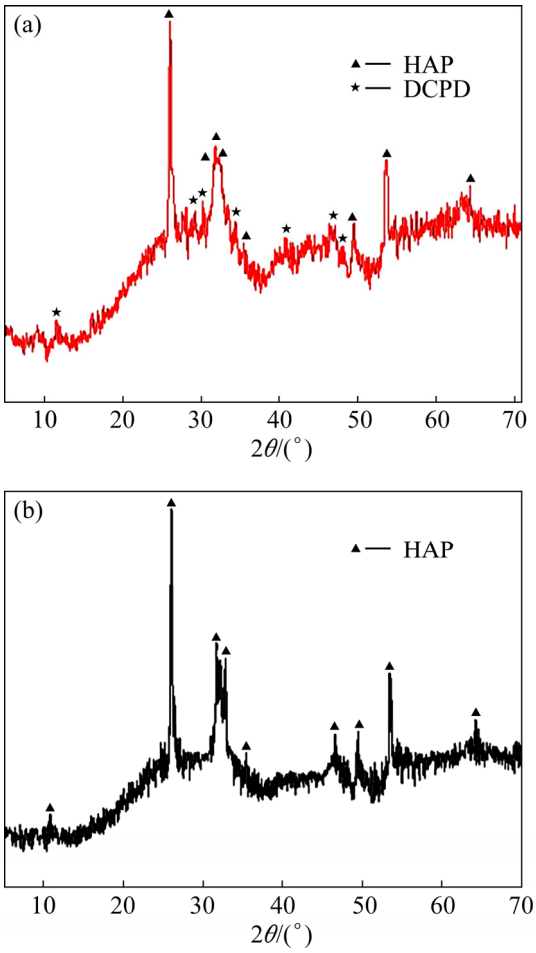

Fig. 4 XRD patterns of as-deposited coating (a) and post-treated coating in alkaline solution (b)

The DCPD formed in the as-deposited coating is converted into HAP after being post-treated with NaOH solution. The following reaction shows the transforming process:

$$10CaHPO_4\cdot 2H_2O+12OH^-\longrightarrow Ca_{10}(PO_4)_6(OH)_2+4PO_4^{3-}+30H_2O \quad (5)$$

During the alkali treatment, the DCPD coating is dissolved releasing Ca^{2+} and PO_4^{3-} ions locally. The nucleation and growth of HA rely on the increased supersaturation. In fact, NaOH solution is used for increasing the pH value. In the alkaline solution such as NaOH, the conversion of DCPD to HAP is promoted due to the favorable thermodynamics and sufficient OH^-. In this system, the transformation will occur without the introduction of additional calcium and phosphate ions, so that it is much easier to trace the conversion processes during the transformation. By the abundant OH^- in the alkaline solution, favorable nucleation sites are provided for the formation of HAP. After nucleation, the HAP crystals then grow outward by consuming the Ca^{2+} and PO_4^{3-} inside the DCPD. The detailed process of HAP crystal growth may involve the dissolution of DCPD, outward diffusion of Ca^{2+} and PO_4^{3-} ions and combination of Ca^{2+} and PO_4^{3-} ions with OH^- ion on the HAP crystal surface to form HAP nano-needles. The crystallization of HAP nano-needles completes via rearranging the orientation.

The SEM images of the as-deposited coating under optimum conditions and the post-treated coating are shown in Figs. 5(a) and (b), respectively. Both of the as-deposited and post-treated coatings exhibit needle-like structure less than 100 nm in diameter. However, the as-deposited coating shows some plate-like structures less than 100 nm in thickness. A small amount of DCPD contained in the as-deposited coating is the possible reason for this morphology difference. Compared with the plate-like surface, the needle-like one may provide more area for the deposition of Ca and P in SBF. In addition, in the post-treated coating, these needles are developed almost perpendicularly to the substrate, with adjacent curled needles fusing together at joint to construct the macroporous structure. It may be beneficial to have a needle-like structure for bone growth, since the inorganic apatite in bone has a needle-shaped morphology with 2−3 nm in thickness and tens of nanometers in length and width [17]. It is known that the bioactivity of apatite highly depends on its composition.

3.3 Immersion testing

In vitro test was performed to evaluate the bioactivity of the coating and the protection capacity of the coating to the scaffold substrate. The specimens were

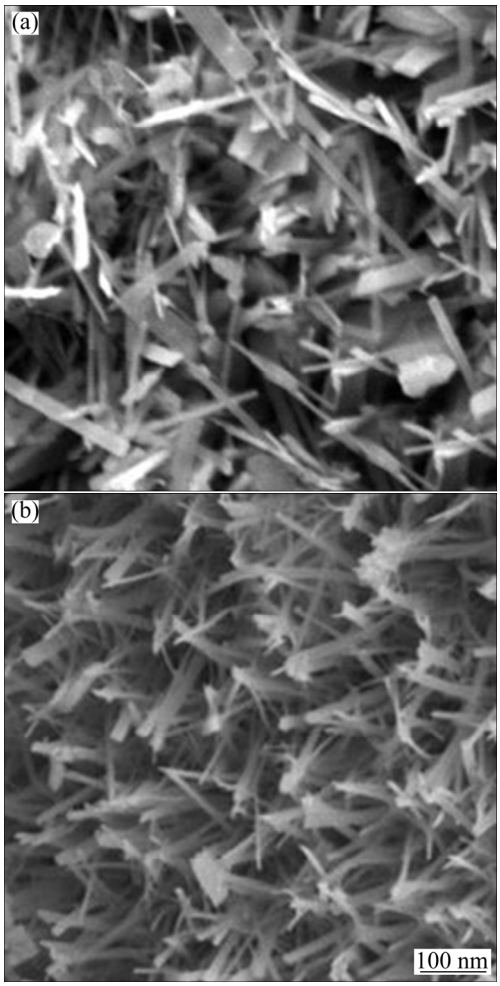

Fig. 5 SEM images of as-deposited coating (a) and post-treated coating by NaOH (b)

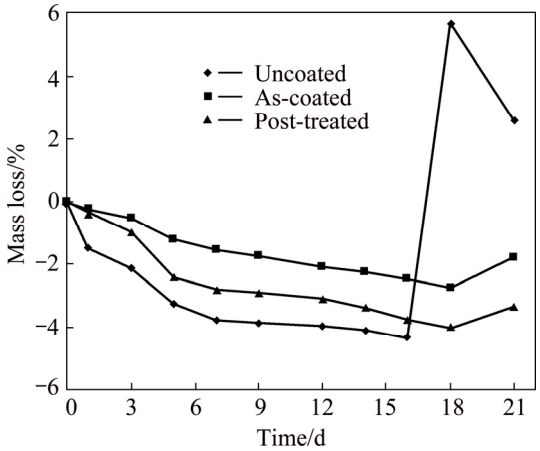

Fig. 6 Mass loss of uncoated, as-coated and post-treated nano-HAP-coated scaffolds immersed in SBF

immersed in SBF for 21 d. Figure 6 shows the variation of mass of the uncoated, as-coated and post-treated scaffolds during the immersions. There is a sharp mass increase for the uncoated scaffold in the first 9 d (Fig. 6). There are some chemical reactions between Mg and SBF. The unprotected porous Mg specimens will develop a gray oxide film of magnesium hydroxide ($Mg(OH)_2$) on the surface of their cell wall which slows degradation [2]. These films of $Mg(OH)_2$ cause the mass of the specimens to increase at the initial stage of immersion. After 9 days' immersion, the mass increase speed is not as fast as before. The possible reason is that the Ca−P−Mg deposit on the Mg alloy substrate would inhibit the further corrosion. There is a sharp mass loss after 16 days' immersion. Although $Mg(OH)_2$ is slightly soluble in water, severe corrosion occurs in aqueous physiological environments, as there is high Cl^- concentration in SBF which causes Mg alloy substrate to be corroded fast, and $Mg(OH)_2$ reacts with Cl^- to form highly soluble magnesium chloride ($MgCl_2$) and H_2 [2].

There is obvious specific mass gain on the as-deposited and post-treated specimens for initial 18 days' immersion. The possible reason is that the concentration of Mg^{2+} in the interface will increase with the corrosion of the substrate. The Mg-rich interface will boost the deposition of Ca−P−Mg apatite. The Ca−P−Mg apatite will increase the thickness of the coating and protect the substrate from further corroding. There is much more mass gain on the post-treated coating than that on the as-deposited coating. Compared with the as-deposited specimen in SBF, the post-treated coating containing pure HAP is much more stable and the needle-like morphology would offer a much larger surface to contact with SBF solution and induce more apatite to the deposit. It can be concluded that the post-treated coating shows better bioactivity.

Figure 7 shows the variations of pH value of the uncoated, as-coated and post-treated scaffolds in SBF solutions during immersions. It can be seen that the pH values of the solutions immersing all of the porous Mg−Zn specimens with and without coating tend to increase in the first 9 d, decrease from 9 to 12 d and then keep at a stable pH value of about 9.65. Mg−Zn scaffolds with Ca−P coating exhibit lower change of pH value and degradation rate in body environment. Mg is converted to Mg^{2+} ions during the degradation process. At the same time, the OH^- ions are released, which causes the pH value of the solutions to increase quickly at early immersion stage. The decrease of pH value from 9 to 12 d should be attributed to the Ca–P coating followed by the formation of the deposited layer. Actually, the pH value of the solutions will keep at stable level when the balance of the formation and dissolution of the deposit is established after about 12 d.

The formed phases on the surface of the uncoated, as-coated and post-treated scaffolds were characterized after the samples were corroded in SBF for 3, 12 and 21 d, respectively, as shown in Fig. 8. The XRD results

confirm that the phases are HAP, $(Ca,Mg)_3(PO_4)_2$ and $Mg(OH)_2$. It can be seen that in the uncoated scaffold, the formed phase is mainly $Mg(OH)_2$, and with the increase of immersion time, the intensities of HAP, $(Ca,Mg)_3(PO_4)_2$ and $Mg(OH)_2$ peaks increase in the as-coated scaffold. Also, the XRD results show that the amount of HAP and $(Ca,Mg)_3(PO_4)_2$ in the as-coated and post-treated scaffolds is more than that in the uncoated scaffold after 21 d.

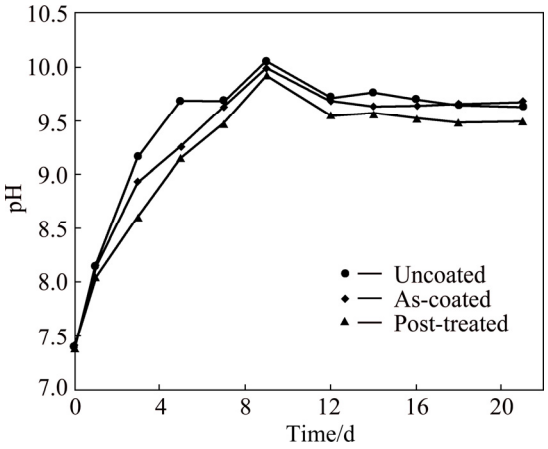

Fig. 7 Change of pH values of SBF solution incubating uncoated, as-coated and post-treated nano-HAP-coated scaffolds during 21 days' immersion

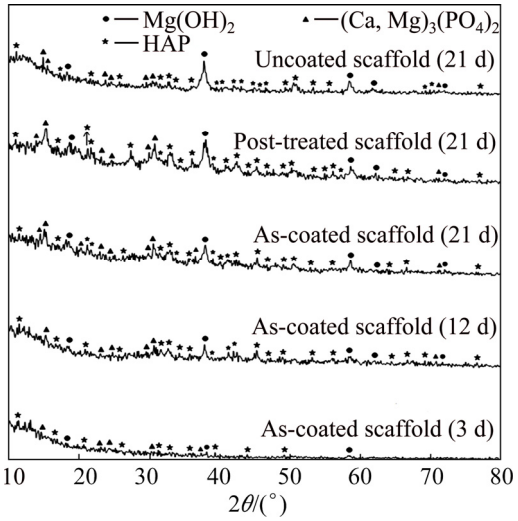

Fig. 8 XRD patterns of uncoated, as-coated and post-treated surface of scaffolds after immersion in SBF for different time

The $Mg(OH)_2$ peak appears at 2θ of 37.5°, indicating the formation of an alkalized layer. The ions in the SBF solution penetrate the HAP coating and reach the scaffolds, leading to further degradation. The dissolution of calcium phosphate compositions leads to the increase of Ca^{2+} and $(PO_4)^{3-}$ concentration near the surface. Therefore, Ca^{2+} and $(PO_4)^{3-}$ ions react with OH^- ions caused from Mg corrosion and form new HAP.

As orthopedic implants, a stable form and a favorable bone–implant interface are especially important during the period of bone remolding. As degradable implants, Mg alloys degrade too fast during the bone remolding period and the precipitated Ca−P minerals will be broken apart by $Mg(OH)_2$, leaving gaps around the Mg implants. Therefore, whether a coating is able to remain intact is a major concern. From the morphology evolution of the Ca−P coatings, it is found that though the HAP needles will not dissolve as quickly as DCPD does, they are prone to dissolve and recrystallize into different textures. A series of studies have demonstrated the interactions between Mg^{2+} and HAP. For instance, there is a critical amount for Mg^{2+}-doped HAP and a higher doping amount will cause the phase transition of HAP [27]. Since Mg^{2+}-incorporated HAP is thermodynamically unstable, the locally accumulated Mg^{2+} may accelerate the decomposition of calcium-deficient hydroxyapatite (Ca-def HAP) by the following reactions: Ca-def HAP$\longrightarrow$$(Ca,Mg)_3(PO_4)_2$ or amorphous Ca−P salts (under high Mg^{2+} concentration).

This fact demonstrates that the coated scaffolds have better bioactivity and osteoconductive. The reason may be that the nano phase of needle-like coating has higher specific surface area, which provides more sites for the absorption of Ca^{2+}, Mg^{2+} and $(PO_4)^{3-}$ from SBF. It was reported that this calcium magnesium phosphate salt had similar chemical composition to natural bone, which showed good bioactivity and osteoconductivity [23]. MENG et al [23] also reported that osteoconductive minerals containing Ca and P could quickly form on the coatings and remain intact for a period of time which was beneficial to increasing the chances for the formation of an osteointegrated interface after implantation.

3.4 Cytotoxicity measurement

Figure 9 shows the cytotoxicity results of uncoated, as-coated and post-treated scaffolds for indirect cell assay using MG63 cells. It can be concluded that the as-coated and post-treated scaffolds extracts indicate improved cell viability, compared with the uncoated scaffold extract. Also, the cell viability obtained in the post-treated scaffold is higher than that obtained in the as-coated scaffold. Furthermore, the post-treated sample shows higher cell viability than the as-coated sample.

Figure 10 shows the morphologies of MG63 cells cultured on the uncoated, as-coated and post-treated scaffolds for 8 h. For the uncoated scaffold, a few cells are observed on the surface after culture for 8 h and unhealthy cells with round shape can be seen. While for the as-coated and post-treated scaffolds, increased cell number with much elongated and healthy cell

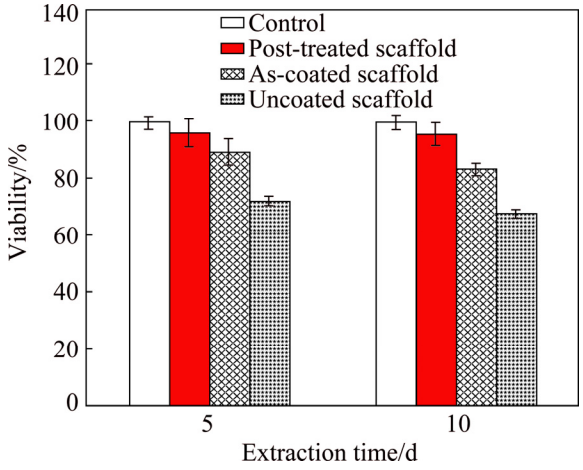

Fig. 9 Cytotoxicity of MG63 cells cultured in uncoated, as-coated and post-treated scaffolds extraction mediums

morphology can be observed. It is noted that the micro-cracks can be seen on the uncoated sample after culture (Fig. 10(a)) and sometime the samples disintegrate into several parts. The results of the indirect cytotoxicity tests show that the present scaffolds exhibit similar cytotoxicity Grades 0–1 (according to ISO 10993-5:1999), which proves their biosafety for further biomedical applications. In the case of the direct assay, the present study indicates well adhered cells on the surface of the as-coated and post-treated scaffold as well as cytotoxicity Grades 0−1. From the comparison of the test results, the as-deposited and post-treated scaffolds exhibit better biocompatibility than the uncoated scaffold. Because the uncoated scaffold is corroded too rapidly, the cells cultured can not adapt to the medium. In the case of coated scaffolds which are corroded slowly with nano HAP, the scaffolds can promote the growth and proliferation of the attached cells. So coating with nano HAP particles is a promising way to improve the biocompatibility of Mg-based materials.

4 Conclusions

1) Nano hydroxyapatite coating with needle-like morphology of less than 100 nm in diameter was obtained by pulse electrodepostion method and post-treatment in NaOH solution to improve the biodegradation behavior of porous Mg−Zn scaffold. The as-deposited coating containing calcium phosphates such as HAP and DCPD and the post-treated coating presenting nano HAP particles were developed almost perpendicularly to the scaffold.

2) The mechanism of formation of HAP coating by electrodeposition involves the reduction of $H_2PO_4^-$ and HPO_4^{2-}, the reaction of PO_4^{3-}, OH^- and HPO_4^{2-} ions

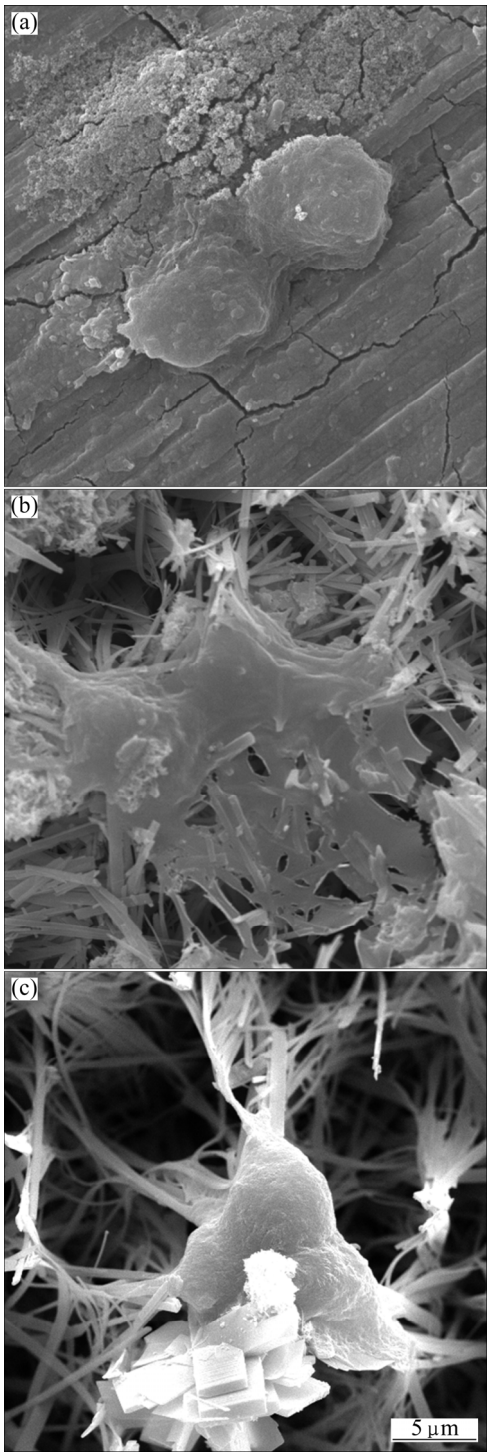

Fig. 10 Morphologies of MG63 cells cultured on uncoated (a), as-coated (b) and post-treated (c) scaffolds for 8 h

with Ca^{2+} ions resulting in the formation of HAP and DCPD, and the conversion of DCPD to HAP. Nano HAP coating can therefore delay the corrosion of the Mg−Zn scaffold in SBF. The results show that the products of immersion in SBF are composed of HAP, $(Ca,Mg)_3(PO_4)_2$ and $Mg(OH)_2$.

3) It is found that the cell viabilities, bioactivity and biocompatibility for the as-coated and post-treated

scaffold extracts are higher than those for the uncoated scaffold. Also, MG63 cells are shown to adhere and proliferate on the surface of as-coated and post-treated scaffolds. Therefore, the pulse electrodeposition of nano HAP coating and post-treatment in alkaline solution is a useful approach to improve the biodegradability and bioactivity of porous Mg−Zn scaffold in SBF and to develop Mg−Zn implants.

References

[1] TAN L, GONG M, ZHENG F, ZHANG B, YANG K E. Study on compression behavior of porous magnesium used as bone tissue engineering scaffold [J]. Biomedical Materials, 2009, 4: 1−7.

[2] ZHUANG H, HAN Y, FENG A. Preparation, mechanical properties and in vitro biodegradation of porous magnesium scaffolds [J]. Materials Science and Engineering C, 2008, 28: 1462−1466.

[3] WEN C E, MABUCHI M, YAMADA Y, SHIMOJIMA K, CHIHO Y, ASAHINA T. Processing of biocompatible porous Ti and Mg [J]. Scripta Materialia, 2001, 45: 1147−1153.

[4] KHANRA A K, JUNG H C, YU S H, HONG K S, SHIN K S. Microstructure and mechanical properties of Mg−HAP composites [J]. Materials Science, 2010, 33: 43−47.

[5] KIRKLAND N T, BIRBILIS N, STAIGER M P. Assessing the corrosion of biodegradable magnesium implants: A critical review of current methodologies and their limitations [J]. Acta Biomaterialia, 2012, 8: 925−936.

[6] LI Z, GU X, LOU S, ZHENG Y. The development of binary Mg−Ca alloys for use as biodegradable materials within bone [J]. Biomaterials, 2008, 29: 1329−1344.

[7] MULLER W D, NASCIMENTO M L, ZEDDIES M, CORSICO M. Magnesium and its alloys as degradable biomaterials: Corrosion studies using potentiodynamic and EIS electrochemical techniques [J]. Materials Research, 2007, 10: 5−10.

[8] WEN C E, YAMADA Y, SHIMOJIMA K, CHINO Y, HOSOKAWA H, MABUCHI M. Compressibility of porous magnesium foam: Dependency on porosity and pore size [J]. Materials Letter, 2004, 58: 357−360.

[9] XIN Y, HUO K, TAO H, TANG G, CHU P K. Influence of aggressive ions on the degradation behavior of biomedical magnesium alloy in physiological environment [J]. Acta Biomaterialia, 2008, 4: 2008−2015.

[10] XIN Y, HU T, CHU P K. Degradation behaviour of pure magnesium in simulated body fluids with different concentrations of HCO_3^- [J]. Corrosion Science, 2011, 53: 1522−1528.

[11] KRAWIEC H, STANEK S, VIGNAL V, LELITO J, SUCHY J S. The use of microcapillary techniques to study the corrosion resistance of AZ91 magnesium alloy at the microscale [J]. Corrosion Science, 2011, 53: 3108−3113.

[12] ATRENS A, LIU M, ABIDIN N I Z. Corrosion mechanism applicable to biodegradable magnesium implants [J]. Materials Science and Engineering B, 2011, 176: 1−28.

[13] WEN C, GUAN S, PENG L, REN C H, WANG X, HU Z. Characterization and degradation behavior of AZ31 alloy surface modified by bone-like hydroxyapatite for implant applications [J]. Applied Surface Science, 2009, 255: 6433−6438.

[14] GUAN R G, JOHNSON I, CUI T, ZHAO T, ZHAO Z Y, LI X, LIU H. Electrodeposition of hydroxyapatite coating on Mg−4.0Zn−1.0Ca−0.6Zr alloy and in vitro evaluation of degradation, hemolysis, and cytotoxicity [J]. Biomedical Materials Research, 2012, 100: 999−1015.

[15] GU X, ZHENG Y, ZHONG S, XI T. Corrosion of, and cellular responses to Mg−Zn−Ca bulk metallic glasses [J]. Biomaterials, 2010, 31: 1093−1103.

[16] KAYA A, ELIEZER D, BEN-HAMU G, GOLAN O, NA Y G, SHIN K S. Microstructure and corrosion resistance of alloys of the Mg−Zn−Ag system [J]. Metal Science and Heat Treatment, 2006, 48: 50−54.

[17] YIN D, ZHANG E, ZENG S. Effect of Zn on mechanical property and corrosion property of extruded Mg−Zn−Mn alloy [J]. Transactions of Nonferrous Metals Society of China, 2008, 18(4): 763−768.

[18] ZHANG E, YIN D, XU L, YANG L, YANG K. Microstructure, mechanical and corrosion properties and biocompatibility of Mg−Zn−Mn alloys for biomedical application [J]. Materials Science and Engineering C, 2009, 29: 987−993.

[19] DUMELIE N, BENHAYOUNE H, RICHARD D, LAURENT-MAQUIN D, BALOSSIER G. In vitro precipitation of electrodeposited calcium-deficient hydroxyapatite coatings on Ti6Al4V substrate [J]. Material Characterization, 2008, 59: 129−133.

[20] SAREMI M, MOTTAGHIGOLSHAN B. Electrodeposition of nano size hydroxyapatite copating on Ti alloy [J]. Iranian Journal of Materials Science and Engineering, 2006, 3: 1−5.

[21] WANG H X, GUAN S K, WANG X, REN C X, WANG L G. In vitro degradation and mechanical integrity of Mg−Zn−Ca alloy coated with Ca-deficient hydroxyapatite by the pulse electrodeposition process [J]. Acta Biomaterialia, 2010, 6: 1743−1748.

[22] SONG Y W, SHAN D Y, HAN E H. Electrodeposition of hydroxyapatite coating on AZ91D magnesium alloy for biomaterial application [J]. Materials Letter, 2008, 62: 3276−3279.

[23] MENG E C, GUAN S K, WANG H X, WANG L G, ZHU S J. Effect of electrodeposition modes on surface characteristics and corrosion properties of fluorine-doped hydroxyapatite coatings on Mg−Zn−Ca alloy [J]. Applied Surface Science, 2011, 257: 4811−4816.

[24] SEYEDRAOUFI Z S, MIRDAMADI S H. Synthesis, microstructure and mechanical properties of porous Mg−Zn scaffolds [J]. Journal of the Mechanical Behavior of Biomedical Materials, 2013, 21: 1−8.

[25] KOKUBO T, TAKADAMA H. How useful is SBF in predicting in vivo bone bioactivity? [J]. Biomaterials, 2006, 27: 2907−2915.

[26] KANNAN M B, RAMAN R K S. In vitro degradation and mechanical integrity of calcium-containing magnesium alloys in modified-simulated body fluid [J]. Biomaterials, 2008, 29: 2306−2314.

[27] SONG Y, ZHANG S H, LI J, ZHAO C H, ZHANG X. Electrodeposition of Ca−P coatings on biodegradable Mg alloy: In vitro biomineralization behavior [J]. Acta Biomaterialia, 2010, 6: 1736−1742.

脉冲电沉积涂覆纳米羟基磷灰石的多孔 Mg−Zn 支架材料的体外生物降解能力和生物相容性

Z. S. SEYEDRAOUFI, Sh. MIRDAMADI

School of Metallurgy and Materials Engineering, Iran University of Science and Technology, Tehran 16846-13114, Iran

摘　要：研究纳米羟基磷灰石(HAP)涂覆的多孔 Mg−2Zn(质量分数，%)支架材料的生物降解能力和生物相容性。采用脉冲电沉积制备羟基磷灰石涂层。对涂覆 HAP 的支架在碱性溶液中进行后处理来改善其生物降解性和生物相容性。研究支架和 HAP 涂层的显微组织和成分以及它们在模拟体液(SBF)中的降解和细胞毒性。经过碱溶液处理后的涂层由几乎垂直于基体的直径小于 100 nm 的针状 HAP 组成，具有和天然骨头相似的成分，浸泡在 SBF 中后，产物为 HAP、$(Ca,Mg)_3(PO_4)_2$ 和 $Mg(OH)_2$。涂覆 HAP 和经过处理碱处理后的支架比未涂覆 HAP 的支架具有更高的生物相容性和细胞存活性。MG63 细胞粘附在涂覆 HAP 和经过碱处理后的支架的表面并增殖，使这些支架有望应用于医学。结果表明：纳米 HAP 的脉冲电沉积和碱处理可有效改善多孔 Mg−Zn 支架的生物降解能力和生物相容性。

关键词：多孔 Mg−Zn 支架；羟基磷灰石涂层；脉冲电沉积；生物降解能力；生物相容性

(Edited by Mu-lan QIN)